Journal of Pediatric Surgery 59 (2024) 161656

Contents lists available at ScienceDirect

Journal of Pediatric Surgery

journal homepage: www.sciencedirect.com/journal/journal-of-pediatric-surgery

Comparative Transcriptome Analysis of Human and Mouse Canalicular Lungs in Fetal Diaphragmatic Hernia

Shelby R. Sferra [1], Juan C. Biancotti [1], Raheel Ahmad, Anne M. Sescleifer, Ciaran R. Bubb, Mark L. Kovler, Shaun M. Kunisaki*

Division of General Pediatric Surgery, Department of Surgery, Johns Hopkins School of Medicine, Baltimore, MD 21287, USA

ARTICLE INFO

Article history:
Received 8 April 2024
Received in revised form
15 July 2024
Accepted 26 July 2024

Keywords:
Congenital diaphragmatic hernia
Transcriptome analysis
Fetal surgery
Animal model

ABSTRACT

Background: The nitrofen model of congenital diaphragmatic hernia (CDH) is widely used in translational research. However, the molecular pathways associated with pulmonary hypoplasia in this model compared to the human CDH phenotype have not been well described. The aim of this study was to investigate differentially expressed genes (DEG) and signaling pathways in early stage fetal lungs in mouse and human CDH.

Methods: CDH lung tissue was obtained from human fetuses (21–23 weeks gestation) and nitrofen mouse pups (E15.5). NovaSeq Flowcell RNA-seq was performed to evaluate differentially expressed transcriptional and molecular pathways (DEGs) in fetal mice with CDH, compared with age-matched normal mouse lungs and human CDH samples.

Results: There were thirteen overlapping DEGs in human and mouse CDH lung samples compared to controls. These genes were involved in extracellular matrix, myogenesis, cilia, and immune modulation pathways. Human CDH was associated with an upregulation of collagen formation and extracellular matrix reorganization whereas mouse CDH was associated with an increase in muscular contraction. The most common cell types upregulated in human and mouse CDH samples were ciliated airway cells.

Conclusions: This study highlights the unique gene transcriptional patterns in early fetal mouse and human lungs with CDH. These data have implications when determining the translational potential of novel therapies in CDH using nitrofen-based animal models.

Level of Evidence: Level IV.

Study Type: Basic science/case series.

1. Introduction

Congenital diaphragmatic hernia (CDH) is a complex, polygenic disorder characterized by incomplete development of a hemidiaphragm with subsequent intrathoracic abdominal organ herniation. All neonates with CDH have bilateral lung hypoplasia with reduced airway branching and alveolar surface area that is more severe on the side of the hernia defect [1]. Despite ongoing advances in prenatal intervention and postnatal care, mortality rates have been stable at 20–25% over the past several decades. Lack of progress in CDH outcomes can be partially attributed to our incomplete understanding of the underlying molecular mechanisms responsible for abnormal lung morphogenesis.

Although several animal models have been used to study CDH lung development, the most widely used model involves the administration of the herbicide 2,4-dichlorophenyl-p-nitrophenyl ether (nitrofen) to pregnant rodents [2]. Studies have shown that the diaphragmatic defects in nitrofen-exposed fetal mice and rats can have comparable anatomy to the human disease phenotype [3]. However, it has been noted that nitrofen-exposed pups develop lung hypoplasia even in the absence of a diaphragmatic defect [4]. Another major criticism of the nitrofen model is that the teratogen has never been shown to induce CDH in humans. It is therefore unclear the extent to which the molecular pathways implicated in nitrofen-exposed fetal lungs may have translational relevance in the clinical arena.

Here, we applied bulk RNA transcriptome analyses to study hypoplastic lungs from mouse and human CDH samples at a similar stage of fetal development. We specifically sought to compare differentially expressed genes (DEGs) and signaling pathways to

Abbreviations: CDH, congenital diaphragmatic hernia; DEG, differentially expressed genes; ECM, extracellular matrix; PCA, principal component analysis.

* Corresponding author. Johns Hopkins School of Medicine Division of General Pediatric Surgery, 1800 Orleans Street, Suite 7353, Baltimore, MD 21287, USA. Tel.: +1 410 955 6256; fax: +1 443 769 1287.
E-mail address: skunisa1@jhmi.edu (S.M. Kunisaki).

[1] These authors contributed equally to this work.

https://doi.org/10.1016/j.jpedsurg.2024.07.041
0022-3468/

understand how the mechanisms behind CDH lung morphogenesis between the two species may be similar or different.

2. Methods

2.1. Human and animal samples

Under an approved materials transfer agreement and Institutional Review Board exempt protocol at the Johns Hopkins School of Medicine, canalicular stage human fetal lung samples from isolated CDH at 21–23 weeks' gestation (n = 2) were obtained from the National Institutes of Health Neurobio bank (University of Maryland, Baltimore, MD, USA). Age-matched normal fetal lungs (n = 2) from the biobank were used as controls. Per database regulations, only gestational age and sex were made available; other patient details including clinical features and laterality of the hernia and lung tissue were not provided.

To induce CDH lung hypoplasia in mice, time-mated pregnant CD1 dams were gavaged at E8.5 with 20 mg nitrofen/5 mg 4-biphenyl carboxylic acid (BPCA, n = 3) [5]. Control dams received corn oil alone (n = 2). Dams were euthanized at E15.5 (late pseudoglandular/early canalicular), entire lungs collected, and total RNA isolated for RNAseq analysis [6]. Whole fetal lungs were collected from control (n = 6) and nitrofen-exposed pups with confirmed large diaphragmatic defects (n = 15). For model validation of nitrofen/BPCA, we also euthanized dams at E17.5 for morphometric analysis of the fetal lungs. This gestational age was chosen exclusively to determine lung/body weight ratio in view of high technical variability in the lung weight taken at E15.5. Animal welfare approval was obtained (MO020M150).

2.2. RNA sequencing analysis

Total RNA was isolated from human and mouse lung samples using the RNeasy plus mini kit (Qiagen Sciences, Germantown, MD, USA), according to the manufacturer's protocol. NEBNext Poly(A) Magnetic Isolation Module (NEB #E7490) and NEBNext Ultra II RNA Library Prep Kit for Illumina (Cat# E7775) were used to generate libraries. Poly A RNAs were isolated from total RNAs and fragmented for cDNA synthesis. End repair was performed where 3′ to 5′ exonuclease activity of enzymes removed 3′ overhangs and the polymerase activity filled in the 5′ overhangs. An 'A' base was then added to the 3′ end of the blunt phosphorylated DNA fragments which prepared the DNA fragments for ligation to the sequencing adapters, which had a single 'T' base overhang at their 3′ end. Ligated fragments were subsequently size selected through purification using the Sample Purification Beads, and PCR amplification techniques were used to prepare the libraries. The BioAnalyzer was used for quality control of the libraries to ensure adequate concentration and appropriate fragment size. The resulting library insert size was 200bp-500bp with a median size around 300bp. Libraries were barcoded using unique dual indexing (E6440S) and pooled for sequencing. Cell type in RNAseq data was implied by contrasting data sets of up- and downregulated gene expression in CDH fetal lungs with a cell atlas obtained from tissue-specific scRNAseq gene expression profiles.

NovaSeq Flowcell RNA-seq, data analysis and validation, and principal component analysis (PCA) were performed on explanted lungs. Nineteen samples were multiplexed, and demultiplexed FASTQ files were generated using bcl-convert v3.7.5.

2.2.1. Quantitative polymerase chain reaction (qPCR)

One microgram of RNA as isolated above were reverse transcribed into cDNA using the Verso cDNA Synthesis kit (Thermo Fisher, Waltham, MA, USA). cDNA was amplified using the PowerUp SYBR Green Master Mix (Thermo Fisher Scientific, Waltham, MA, USA). The mRNA levels of target genes were normalized to glyceraldehyde 3-phosphate dehydrogenase mRNA levels using the $2^{-\Delta\Delta Ct}$ method.

2.2.2. Gene set enrichment and database analysis

The Database for Annotation, Visualization, and Integrated Discovery (DAVID) and Enrichr database were used to assess functional and pathway enrichment analyses [7,8]. DAVID and Enrichr databases were used to systematically derive functional meaning from a large gene list. To determine the role of DEGs in functional analysis, the Gene Ontology (GO) Biological Processes and Reactome 2022 terms were used. Enrichr was also used to analyze cell types through the HuBMap ASCTplusB augmented 2022 terms. Statistical analyses were performed by 2-sided Mann–Whitney Wilcoxon t test or one-way analysis of variance, as appropriate, using Prism 10.1 (GraphPad). DEGs were identified with >2 $\log_{10}$fold change from control, and an adjusted p-value≤0.05 was deemed significant.

3. Results

The rate of diaphragmatic hernia defects in nitrofen-exposed pups was 32% (Fig. 1A). Pulmonary hypoplasia was confirmed at E17.5 based on lung weight adjusted by total body weight (Fig. 1B). In PCA analyses, human CDH and control samples clustered into their respective groups with a PC2 variance of 25% and PC3 variance of 17%. Mouse CDH and control samples at E15.5 had a PC2 variance of 14% and a PC3 variance of 3%. RNA-sequencing in human CDH

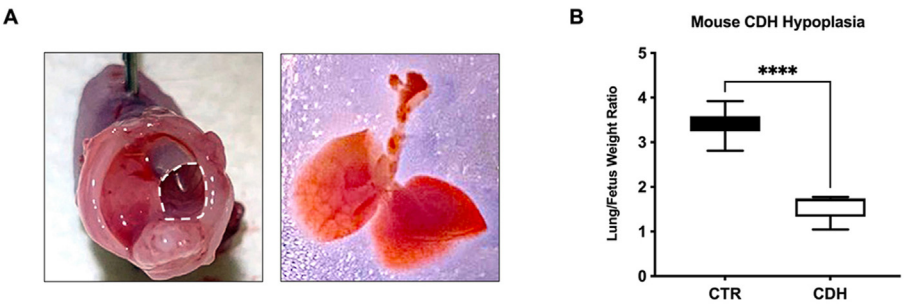

Fig. 1. Human and mouse early canalicular stage lungs in congenital diaphragmatic hernia (CDH) reveal upregulation in mesenchymal and ciliary epithelial pathways. **(A)** Left: transverse section of upper abdomen in nitrofen fetal mouse at E17.5 shows a left posterolateral hernia defect consistent with the human CDH phenotype (white dotted area). Right: Microscopic gross appearance of E17.5 fetal mouse lung explant after nitrofen exposure. **(B)** Box and whiskers plot confirming fetal lung hypoplasia model in E17.5 nitrofen pups with hernia defect (CDH, white) versus age-matched normal lungs receiving control vehicle (CTR, black). Y-axis expressed as a percentage. ****p < 0.0001 (2-sided Mann–Whitney Wilcoxon t test). Error bars are reported as the maximum and minimum.

revealed 493 upregulated and 204 downregulated DEGs. In mouse CDH, there were 333 upregulated and 46 downregulated DEGs from age-matched controls (Fig. 2A).

A heatmap was generated to represent thirteen out of the twenty three overlapping DEGs in human and mouse CDH lung (Fig. 2B). Twenty of the 23 (87%) genes were upregulated in both human and mouse CDH. These DEGs were involved in extracellular matrix (ECM), myogenesis, cilia, and immune modulation pathways. However, human and mouse CDH revealed discordant results in their expression of genes encoding for cell-surface receptors involved in integrin and E-cadherin-mediated signaling pathways. *ITGBL1*, *DUOXA1*, and *CDH16*. *ITGBL1* and *DUOXA1* were upregulated in human CDH but downregulated in mouse CDH. *CDH16*, a gene associated with cadherin binding, was downregulated in human CDH but upregulated in mouse CDH. Confirmation of upregulated genes was corroborated in qPCR analyses (Fig. 2C).

The upregulated transcriptional and molecular pathways were evaluated utilizing Enrichr and DAVID databases (Fig. 3, Table 1). Human CDH was associated with an upregulation of collagen formation, ECM reorganization, and cilia assembly and movement. Mouse CDH was associated with an increase in muscular contraction pathways and cilia assembly/movement. The most common cell types upregulating gene expression in both human and mouse CDH were proximal and distal ciliated cells (Fig. 4).

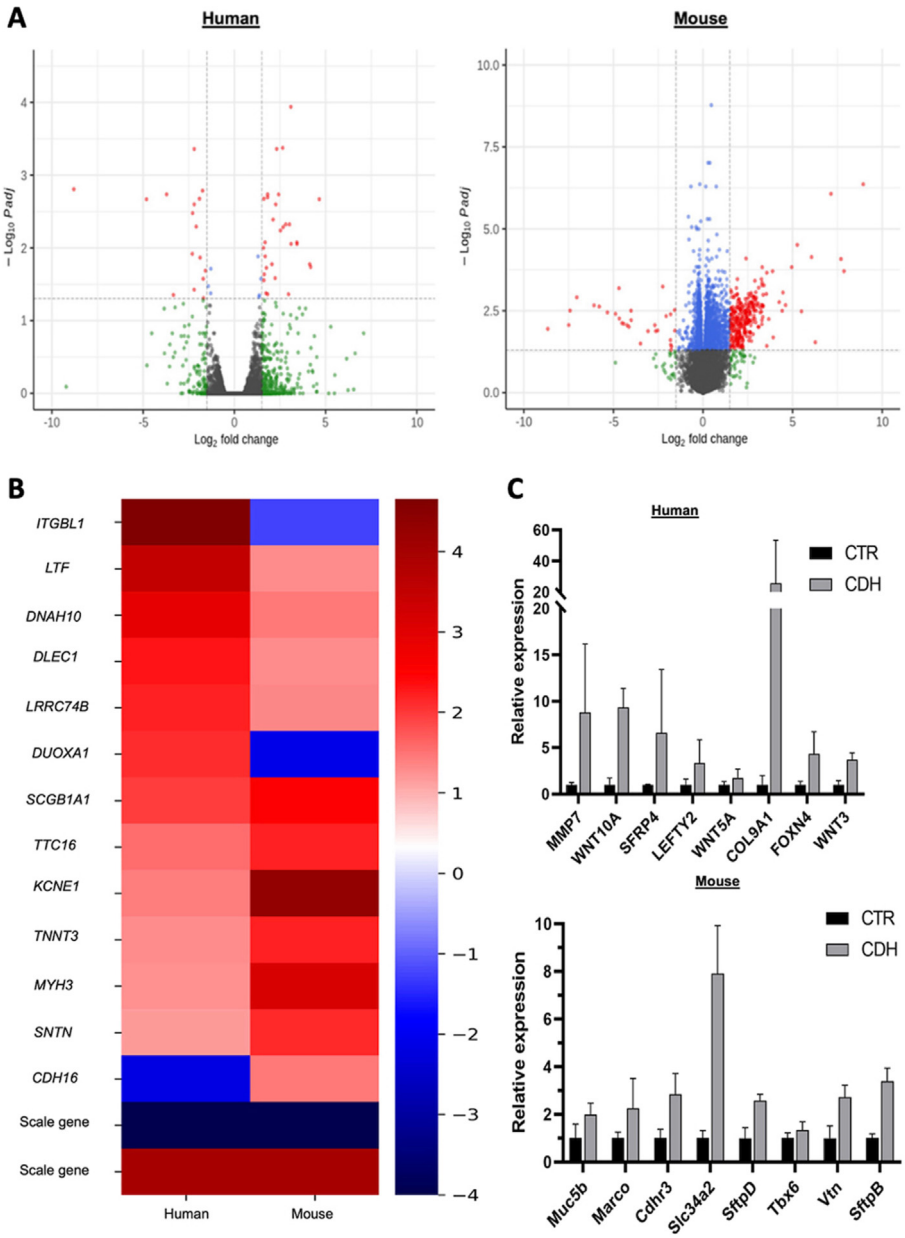

Fig. 2. **(A)** Volcano plots of RNA-seq data showing differentially expressed genes (shown in red) in 21–23 week gestation human CDH lungs (left) and E15.5 nitrofen mouse lungs (right) when normalized by age-matched controls. **(B)** Representative heatmap image shows thirteen overlapping DEGs in human and mouse CDH lungs with >2 log10 fold change. Higher and lower levels of transcripts are shown in red and blue, respectively. Two independent biological replicates. **(C)** Vertical bar graphs confirming quantitative gene expression of 16 upregulated genes in human and mouse CDH lungs based on RNA-seq analysis. Data were normalized relative to housekeeping genes and presented as the mean ± standard deviation, three independent biological replicates, CDH versus control (all $p \leq 0.05$, 2-sided Mann–Whitney Wilcoxon t test). (For interpretation of the references to color in this figure legend, the reader is referred to the Web version of this article.)

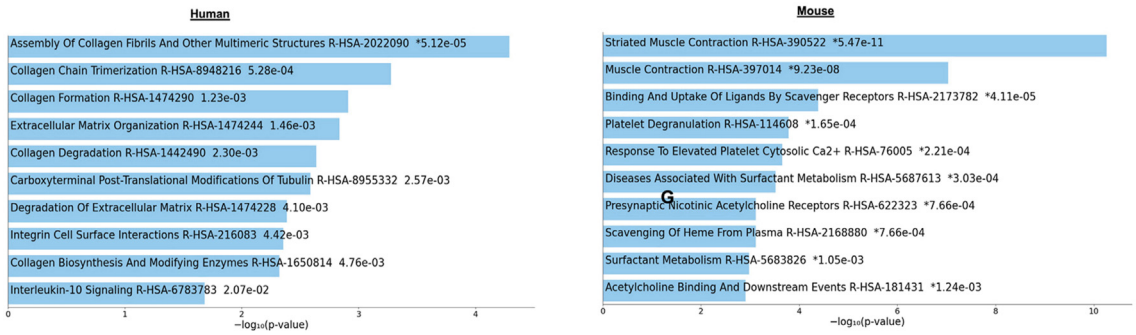

Fig. 3. Transcriptional and molecular pathway analysis revealing an upregulation of collagen formation, extracellular matrix reorganization, and cilia assembly/movement in human CDH as well as an increase in muscular contraction pathways and cilia assembly/movement in nitrofen mouse CDH.

Table 1
Upregulated transcriptional and molecular pathways in canalicular stage fetal lungs from (A) human and (B) nitrofen mice with congenital diaphragmatic hernia, adjusted by age-matched lung controls.

A. Human		
Biologic Process	Odds Ratio	Adjusted *p-value*
Regulation of cilium beat frequency	105.45	4.056e-5
Inner dynein arm assembly	67.92	5.751e-8
Regulation of cilium movement	42.17	3.444e-4
Cilium movement	29.55	6.259e-18
Axonemal dynein complex assembly	22.36	5.751e-8
Axoneme assembly	20.42	7.911e-8
Cilium-dependent cell motility	18.52	1.631e-4
Epithelial cilium involved in extracellular fluid movement	18.11	8.179e-4
Determination of bilateral symmetry	13.47	7.151e-4
Determination of left/right symmetry	13.31	1.180e-5
B. Mouse		
Biologic Process	Odds Ratio	Adjusted *p-value*
Myotube cell development	52.90	8.344e-4
Skeletal muscle contraction	42.72	1.18e-7
Actin-myosin filament sliding	33.85	5.09e-12
Muscle filament sliding	33.85	5.09e-12
Cilium-dependent motility	22.46	1.825e-4
Cilium movement	17.34	1.183e-7
Axoneme assembly	16.55	1.471e-4
Striated muscle contraction	16.53	1.52e-7
Muscle contraction	14.55	8.06e-15
Skeletal muscle tissue development	14.89	2.162e-4

The group of nitrofen-treated mice lacking a diaphragmatic defect but displaying hypoplastic lungs had a transcriptional profile more related to control lungs rather than to CDH lungs as revealed by PCA (Fig. 5). This group had 52 upregulated and 156 downregulated DEGs with respect to control, involved in cilium and cilium movement (upregulated), and in glycoprotein signaling and DNA transcription (downregulated) (Fig. 6A). Comparing hypoplastic lungs without a hernia defect to those with a hernia defect, there was a predominant upregulation of genes in CDH (482 DEGs) and a few downregulated DEGs (19 genes). The upregulated genes were associated with muscular contraction and extracellular space and secretion (Fig. 6B).

4. Discussion

In this novel study, we compared the transcriptome patterns in both human CDH and murine nitrofen-induced CDH at a similar stage of pulmonary development (early canalicular). Of note, hypoplastic lungs from nitrofen-exposed pups without a diaphragmatic hernia were also analyzed separately, demonstrating an intermediate phenotype similar to control lungs but distinct from lungs with a defect. In view of this, we elected to focus only on fetal mice with a defect in this study in an attempt to more closely parallel the human phenotype.

Our study found that both humans and mice with CDH demonstrated aberrant pulmonary development in the early canalicular stage, characterized by a profound upregulation in genes corresponding to tracheal and bronchial ciliated cells. Others have shown increased calcitonin gene-related peptide and forkhead box J1 genes, markers of neuroendocrine and ciliated cells, respectively, in the terminal bronchioles of CDH [9]. These data are also consistent with a common, aberrant proximal-distal epithelial patterning observed in a human CDH lung organoid model [10]. The involvement of compression over lung development was addressed comparing lungs from nitrofen mice with and without diaphragm defect. These transcriptome data suggest that compression itself affects muscle and ECM development within the lung and thus contribute to the pathogenesis of CDH.

The upregulation of various ECM genes within the mesenchyme has been implicated as the mechanism for the reduced pulmonary compliance and the increased pulmonary arterial hypertension seen in CDH [11,12]. Our data also suggest that the primary dysregulation in human CDH is marked by upregulation of the ECM-related genes, whereas genes associated with muscle hypercontractility were enhanced in the nitrofen mouse model. The mouse transcriptome data are consistent with mechanistic descriptions of CDH pathogenesis based on the smooth muscle hypothesis, in which signaling from the pleuroperitoneal folds results in aberrant lung morphogenesis [13,14]. We also found discordant DEGs associated with integrin, neurogenesis and E-cadherin signaling pathways. Interestingly, genes enriched for integrin and neurogenesis annotations have also been distinctively expressed in a mouse strain-dependent manner during normal lung development [15]. Moreover, there are DEGs in normal lung development that lack homology between mouse and human, and from those homologous DEGs the overlap between mouse and human lung development genes is only a small fraction of the total transcriptome.

Both human and nitrofen mouse CDH have phenotypic similarities within the mesenchymal compartment, but some of the mechanistic pathways underlying aberrant lung morphogenesis are likely unique. Our findings are consistent with those reported by others, demonstrating mesenchymal dysregulation as a major driving force for CDH lung hypoplasia [16–19]. Taken together, these results suggest that compression derived from the herniation of viscera into the thoracic cavity may have a profound effect on promoting the development of lung musculature, and the extracellular matrix and cell signaling. Overall, in view of the similarities

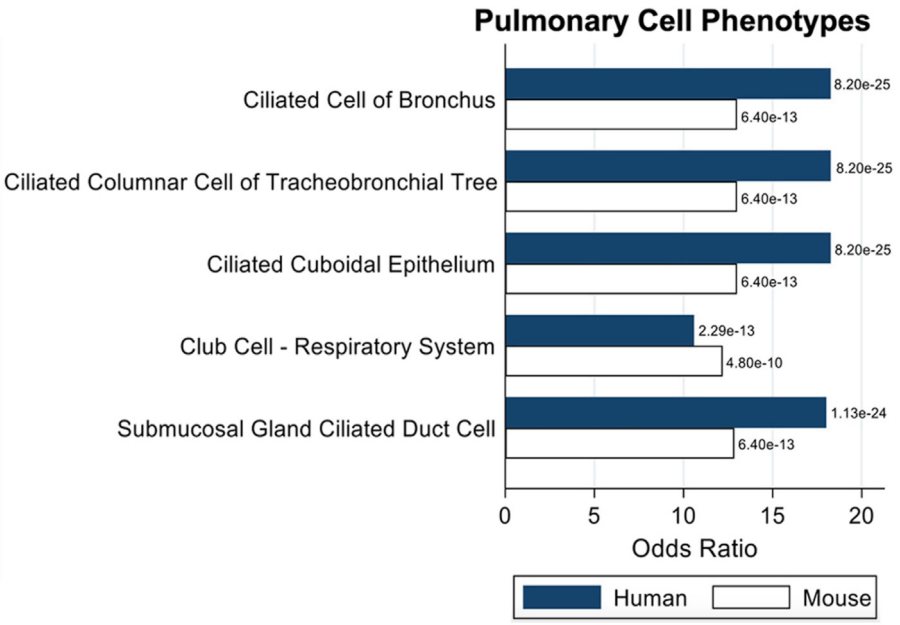

Fig. 4. Analysis using the Enrichr database identified proximal and distal ciliated cells as the most common cell types upregulated in both human and nitrofen mouse CDH when normalized by age-matched normal controls.

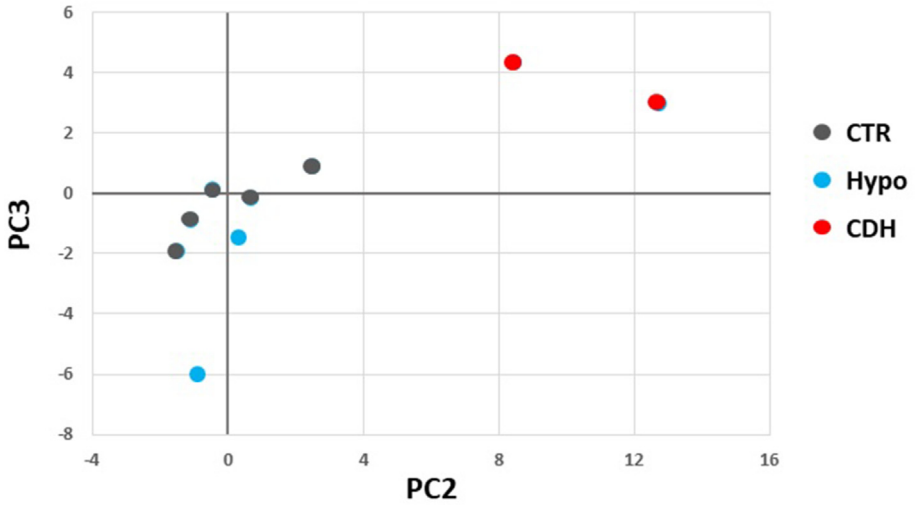

Fig. 5. Principal Component Analysis plot of mouse lungs subgroups. PC2 (14% variance) and PC3 (3% variance) for control (CTR), nitrofen-treated mice without diaphragm defect (Hypo), and nitrofen-treated mice with diaphragm defect (CDH). CTR cluster together and very close with Hypo, but apart from CDH.

in the affected biological processes and cell types emerging from the transcriptome data, we consider that the nitrofen mouse is a valuable model of human CDH.

Based on these transcriptome data, we hypothesize that pharmacologic approaches that can modulate the proximal-distal epithelial axis pathway may represent a novel therapeutic target to combat lung hypoplasia in human CDH [20]. However, care must be taken not to overstate the results from these analyses due to several limitations. First, additional studies in human CDH lungs are needed to evaluate inherent genetic variations and other patient-specific factors since we only had access to a limited number of human specimens at the appropriate gestational age. Confirmation of our findings at the cellular and/or protein level would also be desirable. Furthermore, our analysis was limited by lack of relevant clinical data correlating to the human samples, including laterality of lung tissue and clinical severity of CDH. In addition, pooling of both right and left lung samples may have blunted the DEG signals, as the ipsilateral lung is known to be more severely hypoplastic in CDH, and the validity of these results may be restricted since our data were derived from a nitrofen/BPCA mouse model as opposed to the more widely studied nitrofen rat model of CDH. Finally, we examined alterations in DEGs during the early canalicular stage when normal diaphragm closure has already occurred. Genes involving immunomodulation, among other critical signaling pathways, may be dysregulated during earlier or later stages of CDH fetal lung development [21].

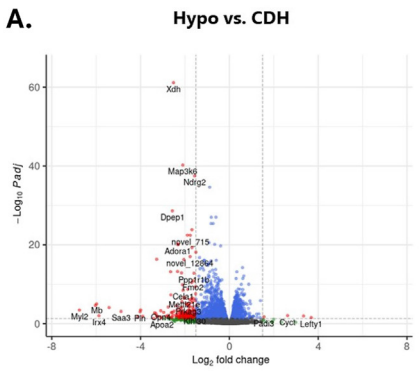

Annotation cluster 1	Enrichment score: 13.26	Count	P-value	Benjamini
GOTERM_BP_DIRECT	cardiac muscle contraction	19	1.10E-18	8.20E-16
KEGG_PATHWAY	Hypertrophic cardiomyopathy	23	5.60E-17	1.40E-14
Annotation cluster 2	**Enrichment score: 9.77**	**Count**	**P-value**	**Benjamini**
GOTERM_CC_DIRECT	extracellular region	89	1.30E-15	1.10E-13
UP_KW_CELLULAR_COMPONENT	Secreted	80	4.30E-13	1.40E-11
GOTERM_CC_DIRECT	extracellular space	85	5.60E-13	2.10E-11
Annotation cluster 3	**Enrichment score: 9.58**	**Count**	**P-value**	**Benjamini**
GOTERM_CC_DIRECT	sarcoplasmic reticulum	19	4.00E-15	2.90E-13
KEGG_PATHWAY	Calcium signaling pathway	21	4.20E-07	1.80E-05
Annotation cluster 4	**Enrichment score: 7.38**	**Count**	**P-value**	**Benjamini**
UP_KW_MOLECULAR_FUNCTION	Muscle protein	32	7.70E-38	5.80E-36
GOTERM_BP_DIRECT	muscle contraction	21	2.70E-21	2.90E-18
GOTERM_BP_DIRECT	cardiac muscle contraction	19	1.10E-18	8.20E-16

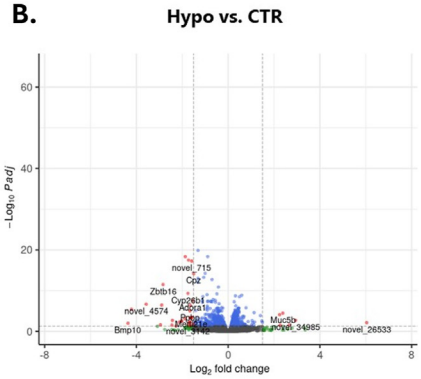

Annotation cluster 1	Enrichment score: 4.19	Count	P-value	Benjamini
UP_KW_PTM	Glycoprotein	47	4.00E-07	6.70E-06
UP_KW_PTM	Disulfide bond	37	9.10E-05	7.70E-04
Annotation cluster 2	**Enrichment score: 2.1**	**Count**	**P-value**	**Benjamini**
GOTERM_MF_DIRECT	RNA polymerase II regulatory re	12	2.50E-05	6.30E-03
INTERPRO	Homeobox_CS	8	7.80E-05	3.20E-02

Fig. 6. Compression impairs lung development in nitrofen-treated lungs. **(A)** Volcano plot of DEGs from hypoplastic versus control (Hypo vs. CTR) groups, and annotation clusters corresponding to downregulated DEGs in hypoplastic lungs. **(B)** Volcano plot of DEGs from hypoplastic versus CDH (Hypo vs. CDH) groups, and annotation clusters corresponding to CDH upregulated (Hypo downregulated) DEGs. Annotation clusters were obtained by analysis of DEGs using DAVID Bioinformatic tool. Significance denotes >2-fold change, p-value≤0.05).

Financial Support statement

This work was funded by the Barnes Research Fund, an internal award provided by the Department of Surgery at Johns Hopkins School of Medicine. The funder had no role in the design, data collection, data analysis, and reporting of this study.

Conflicts of interest

The authors have no conflicts of interest to declare.

Acknowledgements

We thank Dr. Liliana Florea and Corina Antonescu from the Computational Biology Consulting Core at Johns Hopkins Medicine for advice and contribution towards the execution and analysis of our transcriptomics work.

References

[1] Zani A, Chung WK, Deprest J, Harting MT, Jancelewicz T, Kunisaki SM, et al. Congenital diaphragmatic hernia. Nat Rev Dis Prim 2022;8(1):37. https://doi.org/10.1038/s41572-022-00362-w. Epub 2022/06/02. PubMed PMID: 35650272.

[2] Kluth D, Kangah R, Reich P, Tenbrinck R, Tibboel D, Lambrecht W. Nitrofen-induced diaphragmatic hernias in rats: an animal model. J Pediatr Surg 1990;25(8):850–4. https://doi.org/10.1016/0022-3468(90)90190-k. Epub 1990/08/01. PubMed PMID: 2401939.

[3] van Loenhout RB, Tibboel D, Post M, Keijzer R. Congenital diaphragmatic hernia: comparison of animal models and relevance to the human situation. Neonatology 2009;96(3):137–49. https://doi.org/10.1159/000209850. Epub 2009/03/28. PubMed PMID: 19325248.

[4] Guilbert TW, Gebb SA, Shannon JM. Lung hypoplasia in the nitrofen model of congenital diaphragmatic hernia occurs early in development. Am J Physiol Lung Cell Mol Physiol 2000;279(6):L1159–71. https://doi.org/10.1152/ajplung.2000.279.6.L1159. Epub 2000/11/15. PubMed PMID: 11076806.

[5] Kool HM, Burgisser PE, Edel GG, de Kleer I, Boerema-de Munck A, de Laat I, et al. Inhibition of retinoic acid signaling induces aberrant pericyte coverage and differentiation resulting in vascular defects in congenital diaphragmatic hernia. Am J Physiol Lung Cell Mol Physiol 2019;317(3):L317–31. https://doi.org/10.1152/ajplung.00104.2018. Epub 2019/07/04. PubMed PMID: 31268349.

[6] Gouveia L, Betsholtz C, Andrae J. Expression analysis of platelet-derived growth factor receptor alpha and its ligands in the developing mouse lung. Physiol Rep 2017 Mar;5(6):e13092. https://doi.org/10.14814/phy2.13092. PMID: 28330949; PMCID: PMC5371545.

[7] Huang da W, Sherman BT, Lempicki RA. Systematic and integrative analysis of large gene lists using DAVID bioinformatics resources. Nat Protoc 2009;4(1):44–57. https://doi.org/10.1038/nprot.2008.211. Epub 2009/01/10. PubMed PMID: 19131956.

[8] Kuleshov MV, Jones MR, Rouillard AD, Fernandez NF, Duan Q, Wang Z, et al. Enrichr: a comprehensive gene set enrichment analysis web server 2016 update. Nucleic Acids Res 2016;44(W1):W90–7. https://doi.org/10.1093/nar/gkw377. Epub 2016/05/05. PubMed PMID: 27141961; PubMed Central PMCID: PMCPMC4987924.

[9] Goncalves AN, Correia-Pinto J, Nogueira-Silva C. Distinct epithelial cell profiles in normal versus induced-congenital diaphragmatic hernia fetal lungs. Front Pediatr 2022;10:836591. https://doi.org/10.3389/fped.2022.836591. Epub 2022/05/24. PubMed PMID: 35601428; PubMed Central PMCID: PMCPMC9120630.

[10] Kunisaki SM, Jiang G, Biancotti JC, Ho KKY, Dye BR, Liu AP, et al. Human induced pluripotent stem cell-derived lung organoids in an ex vivo model of the congenital diaphragmatic hernia fetal lung. Stem Cells Transl Med 2021;10(1):98–114. https://doi.org/10.1002/sctm.20-0199. Epub 2020/09/20. PubMed PMID: 32949227; PubMed Central PMCID: PMCPMC7780804.

[11] Wild B, St-Pierre ME, Langlois S, Cowan KN. Elastase and matrix metalloproteinase activities are associated with pulmonary vascular disease in the nitrofen rat model of congenital diaphragmatic hernia. J Pediatr Surg 2017;52(5):693–701. https://doi.org/10.1016/j.jpedsurg.2017.01.010. Epub 2017/02/13. PubMed PMID: 28189447.

[12] Montalva L, Antounians L, Zani A. Pulmonary hypertension secondary to congenital diaphragmatic hernia: factors and pathways involved in pulmonary vascular remodeling. Pediatr Res 2019;85(6):754–68. https://doi.org/10.1038/s41390-019-0345-4. Epub 2019/02/20. PubMed PMID: 30780153.

[13] Featherstone NC, Connell MG, Fernig DG, Wray S, Burdyga TV, Losty PD, et al. Airway smooth muscle dysfunction precedes teratogenic congenital

diaphragmatic hernia and may contribute to hypoplastic lung morphogenesis. Am J Respir Cell Mol Biol 2006;35(5):571–8. https://doi.org/10.1165/rcmb.2006-0079OC. Epub 2006/05/27. PubMed PMID: 16728706.

[14] Jesudason EC. Small lungs and suspect smooth muscle: congenital diaphragmatic hernia and the smooth muscle hypothesis. J Pediatr Surg 2006;41(2):431–5. https://doi.org/10.1016/j.jpedsurg.2005.11.021. Epub 2006/02/17. PubMed PMID: 16481264.

[15] Beauchemin KJ, Wells JM, Kho AT, Philip VM, Kamir D, Kohane IS, Graber JH, Bult CJ. Temporal dynamics of the developing lung transcriptome in three common inbred strains of laboratory mice reveals multiple stages of postnatal alveolar development. PeerJ 2016 Aug 9;4:e2318. https://doi.org/10.7717/peerj.2318. PMID: 27602285; PMCID: PMC4991849.

[16] Perveen S, Frigeni M, Benveniste H, Kurepa D. Cellular, molecular, and metabolic aspects of developing lungs in congenital diaphragmatic hernia. Front Pediatr 2022 Nov 15;10:932463. https://doi.org/10.3389/fped.2022.932463. PMID: 36458148; PMCID: PMC9706094.

[17] van Loenhout RB, Tseu I, Fox EK, Huang Z, Tibboel D, Post M, Keijzer R. The pulmonary mesenchymal tissue layer is defective in an in vitro recombinant model of nitrofen-induced lung hypoplasia. Am J Pathol 2012 Jan;180(1):48–60. https://doi.org/10.1016/j.ajpath.2011.09.032. Epub 2011 Nov 4. PMID: 22063298.Y.

[18] Y Ornitz DM, editor. FGF9 and FGF10 activate distinct signaling pathways to direct lung epithelial specification and branching. Sci Signal 2020 Mar 3;13(621):eaay4353. https://doi.org/10.1126/scisignal.aay4353. PMID: 32127497; PMCID: PMC7271816.

[19] Yin Y, Wang F, Ornitz DM. Mesothelial- and epithelial-derived FGF9 have distinct functions in the regulation of lung development. Development 2011 Aug;138(15):3169–77. https://doi.org/10.1242/dev.065110. PMID: 21750028; PMCID: PMC3188607.

[20] Lange AW, Sridharan A, Xu Y, Stripp BR, Perl AK, Whitsett JA. Hippo/Yap signaling controls epithelial progenitor cell proliferation and differentiation in the embryonic and adult lung. J Mol Cell Biol 2015;7(1):35–47. https://doi.org/10.1093/jmcb/mju046. Epub 2014/12/07. PubMed PMID: 25480985; PubMed Central PMCID: PMCPMC4400400.

[21] Dylong F, Riedel J, Amonkar GM, Peukert N, Lieckfeldt P, Sturm K, et al. Overactivated epithelial NF-kappaB disrupts lung development in congenital diaphragmatic hernia. Am J Respir Cell Mol Biol 2023. https://doi.org/10.1165/rcmb.2023-0138OC. Epub 2023/08/08. PubMed PMID: 375528.